

- JOHNSON, C. K. (1965). *ORTEP*. Oak Ridge National Laboratory Report ORNL-3794.
- KOLLMAN, P. (1974). *J. Amer. Chem. Soc.* **96**, 4363–4369.
- MERCER, M. & TRUTER, M. R. (1973). *J. Chem. Soc. Dalton*, pp. 2215–2220.
- PAULING, L. (1960). *The Nature of the Chemical Bond*. New York: Cornell Univ. Press.
- PEDERSEN, C. J. (1967). *J. Amer. Chem. Soc.* **89**, 7017–7036.
- PEDERSEN, C. J. & FRENSDORFF, H. K. (1972). *Angew. Chem. Int. Ed.* **11**, 16–25.
- ROBB, M. A., HAINES, W. J. & CSIZMADIA, I. G. (1973). *J. Amer. Chem. Soc.* **95**, 42–48.
- RUYSINK, A. F. J. & VOS, A. (1974). *Acta Cryst.* **A30**, 503–506.
- SIMON, W. & MORF, W. E. (1973). In *Membranes*, Vol. 2, edited by G. EISENMAN, pp. 329–375. New York: Marcel Dekker.
- SIMON, W., MORF, W. E. & MEIER, P. C. (1973). *Struct. Bond.* **16**, 113–160.
- STEWART, R. F., DAVIDSON, E. R. & SIMPSON, W. T. (1965). *J. Chem. Phys.* **42**, 3175–3187.
- STROUSE, C. E. (1974). To be published.
- Tables of Interatomic Distances and Configuration in Molecules and Ions* (1960). Spec. Publ. No. 18. London: The Chemical Society.
- TRUTER, M. R. (1973). *Struct. Bond.* **16**, 71–111, and references cited therein.
- WILSON, A. J. C. (1949) *Acta Cryst.* **2**, 318–321.

Acta Cryst. (1975). **B31**, 762

Structural and E.p.r. Search for Exchange Striction in Pyrazine Copper Acetate*

BY B. MOROSIN AND R. C. HUGHES

Sandia Laboratories, Albuquerque, New Mexico 87115, U.S.A.

AND Z. G. SOOS

Department of Chemistry, Princeton University, Princeton, New Jersey 08540, U.S.A.

(Received 23 September 1974; accepted 21 October 1974)

The crystal structure of pyrazine copper acetate ($\text{Cu}_2\text{Ac}_4 \cdot \text{pyrazine}$), a binuclear copper acetate system in which the Cu–Cu separation in the triplet state has been estimated to be 0.12 Å longer than that in the singlet state, has been determined and refined by least-squares methods using three-dimensional Mo $K\alpha$ data (to $57^\circ 2\theta$) at 298 and 100 K. In a complementary study of possible exchange striction in this singlet-triplet system, 35 GHz (Q -band) e.p.r. spectra were measured at 298 and 120 K. Pyrazine copper acetate crystallizes in space group $C2/m$ in a cell of dimensions $a = 7.967$ (19), $b = 14.211$ (1), $c = 7.3210$ (8) Å and $\beta = 101.23$ (2)° at 298 K and $a = 7.9156$ (9), $b = 14.025$ (3), $c = 7.3022$ (9) Å and $\beta = 100.99$ (2)° at 100 K. The 298 K Cu–Cu separation of 2.583 (1) Å is significantly shorter than those found in similar dimer compounds and is only 0.007 Å longer than at 100 K. The small changes in the e.p.r. fine structure observed at 298 and 120 K show that the exchange in the excited state changes by less than 1% and suggest a constant Cu–Cu separation in the triplet state, as occurs in an exchange-striction model. The single-crystal e.p.r. also provides an experimental separation of the fine structure into spin-orbit and dipolar contributions.

Introduction

Recently the crystal structures and phase transitions of several linear-chain magnetic systems (Bartkowski & Morosin, 1972; Peercy, Morosin & Samara, 1973; Richards, Quinn & Morosin, 1973) have been examined. These systems consist of chemically bonded transition-metal ions arranged equidistant from each other with separations within the chain much smaller than those between the chains. Pyrazine copper acetate (PzCuAc), represents a different, novel linear-chain complex in which binuclear copper acetate units, $\text{Cu}_2(\text{CH}_3\text{CO}_2)_4$, are linked by the pyrazine ligand, $\text{C}_4\text{H}_4\text{N}_2$. This system was first prepared and studied by Valentine, Silverstein & Soos (1974), hereinafter referred to as VSS.

Binuclear copper clusters are known in quite a few other copper alkanoates and carboxylates (Martin, 1968; Kokoszka & Gordon, 1969). The magnetic properties of such binuclear clusters have been intensively studied by static susceptibility and e.p.r. measurements. Typically one finds a rather strong antiferromagnetic exchange interaction, J , within the cluster, with $|J|$ of the order of 400K. However, the exchange interaction between clusters, J' , is much smaller and more difficult to measure and interpret since very low temperatures are required and in such temperature regions, other approximations are suspect. A further complication results if J' is of the same order as the electron dipolar interactions between clusters; then even n.m.r. measurements may prove unable to distinguish between intercluster exchange and dipolar contributions. Such is the case for the familiar hydrate of copper acetate, HyCuAc (Obata, 1967).

* Supported in part by the USAEC and by NSF GP-9546.

The bidentate pyrazine ligand was used in VSS as a chemical bridge between the copper acetate units, thus providing a clustered system with some linear-chain properties. The chain structure is $\dots\text{Cu}-\text{Cu}-\text{N}(\text{C}_4\text{H}_4)\text{N}-\text{Cu}-\text{Cu}\dots$ and all the chains are parallel. The intercluster exchange J' was found to be about 1100G from the temperature-dependent broadening of the e.p.r. lines and is one to two orders of magnitude larger than interdimer dipolar fields. The resolved hyperfine structure at 77K, on the other hand, placed a smaller limit of less than 30G (80MHz) on the exciton motion. This observation is consistent with an exchange-striction mechanism for the case where the lower rate of exciton motion arises from a reduction of J' due to the Franck-Condon overlap of the copper nuclei in the singlet and triplet states. Although binuclear copper complexes may well have different Cu-Cu stretching frequencies in the singlet and triplet state (Martin, 1966), the estimate of $\hbar\omega = 100\text{ cm}^{-1}$ for both yielded a predicted difference of 0.12 Å for the Cu-Cu separation in the singlet and in the triplet state.

A fractional part of this difference, based on the change in the thermal-equilibrium triplet density, should be observable in carefully determined structures using low- and room-temperature data. Using the observed exchange $J = 460\text{K}$, we plot in Fig. 1 the number of triplets as a function of reciprocal temperature. The

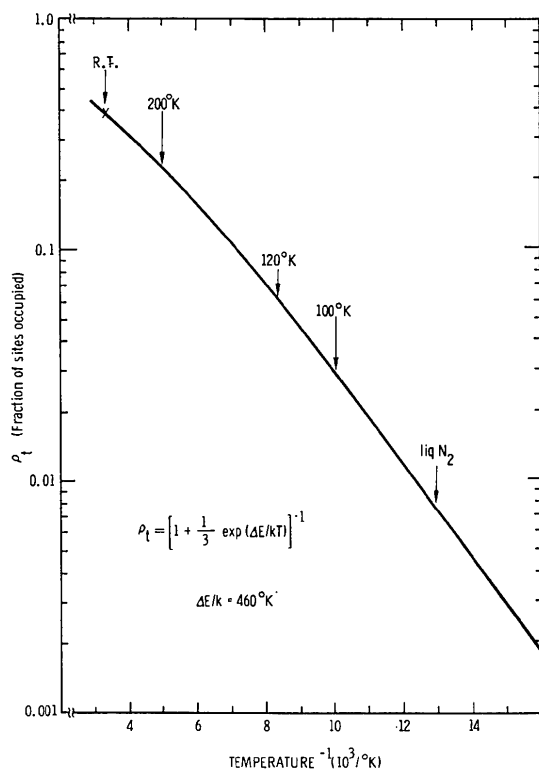


Fig. 1. Plot of expected number of triplets versus reciprocal temperature. At room temperature, about 40% of the sites should occupy the triplet state; temperatures near liquid nitrogen are needed to reduce the population of triplets below 1%.

difference between the room-temperature triplet density of about 40% and the 100K density of 3% was anticipated to produce at least a 0.04 Å change in the Cu-Cu separation. The close similarity of the CuAc dimer in PzCuAc to other binuclear CuAc compounds (Kokoszka & Gordon, 1969) suggested that such exchange striction, if observed in one compound, would be a general property of the class. The linear-chain structure of PzCuAc, with all Cu-Cu vectors parallel, provides experimental advantages and was chosen for both X-ray and further e.p.r. investigations.

We report here structural and e.p.r. studies on PzCuAc at 298 and at 100K. The unexpected structural results include a Cu-Cu separation at room temperature that is significantly shorter than in similar dimer clusters. The observed contraction of the Cu-Cu distance is, furthermore, only 0.007 (1) Å and thus far smaller than the estimated 0.04 Å change indicated in VSS. Recent improved theoretical work on polaron motion (Emin, 1974) suggests that a smaller striction would be consistent with the observed absence of triplet motion at low temperature. The question of whether there is exchange striction in PzCuAc remains unresolved, however, since the observed structural changes are small enough to be attributed to thermal expansion.

Thermal expansion requires that all Cu-Cu separations be equal at any temperature. Exchange striction leads to two Cu-Cu separations, one for triplets and a shorter one for singlet dimers, with the change of 0.007 Å between 300 and 100K, requiring a striction of 0.02 Å. While structural data provide the average Cu-Cu separation as a function of temperature, e.p.r. studies monitor only the Cu-Cu separation in the triplet dimers. The temperature dependence of the high-field (*Q*-band) spectra thus complements structural studies and, as shown below, permits an experimental separation of spin-orbit and dipolar contributions to the fine-structure splitting. The absence of significant fine-structure changes between 300 and 120K indicates that the excited-state exchange interactions change by less than 1% and supports an exchange-striction model, with a nearly constant Cu-Cu separation in the triplet state, since exchange interaction can be sensitive to even small changes in the internuclear separation (Morosin, 1970). The present structural and magnetic study of the temperature dependence of the Cu-Cu separation in PzCuAc shows that, while thermal expansion cannot be ruled out, a consistent interpretation of the data may be made employing a model with a small exchange striction.

Experimental details

Precession and Weissenberg photographs were used to determine preliminary unit-cell dimensions and space-group extinctions. In addition photographic methods were used to examine the quality of the data crystal at low temperatures as well as those undergoing several

cooling temperature excursions. At both 298 and 100K temperatures, identical systematic absences and symmetries of the reciprocal lattice were found, indicating the space group to be $C2$, Cm or $C2/m$. Low temperatures on both film and diffractometer units were achieved using a Varian variable-temperature controller, which regulates the temperature of a nitrogen gas stream over the crystal specimen. Lattice constants (Table 1) were determined by least-squares fit of 2θ values measured on a Picker diffractometer using $Cu K\alpha$ radiation ($\lambda_{\alpha_1} = 1.54050 \text{ \AA}$). Cleaved and solvent-eroded samples with no dimension greater than 0.03 cm were used for lattice parameters and intensity measurements. The θ - 2θ scan technique and scintillation detector employing pulse height discrimination were used to measure $Mo K\alpha$ intensity data sets to $57^\circ 2\theta$. (Data for the 100K set were collected in four concentric shells and computer round-off errors resulted in a few hkl intensities never being collected; such absences were discovered only recently.) Intensity data measured to be less than 3σ were considered as unobserved reflections. The usual definition of σ was used, *i.e.* $\sigma = (N_{sc} + K^2 N_b)^{1/2}$ and N_{sc} , N_b , and K (≈ 4 -5) are the total scan count, background counts (20 s on each side of the scan), and time ratio of the scan to background, respectively.

Table 1. Cell dimensions for $PzCuAc$

| Probable space group: $C2/m$ | | |
|------------------------------|--------------------------|--------------------------|
| | 300K | 100K |
| a | 7.9671 (9) \AA | 7.9156 (9) \AA |
| b | 14.211 (1) | 14.025 (3) |
| c | 7.3210 (8) | 7.3022 (9) |
| β | 101.23 (2) $^\circ$ | 100.99 (2) $^\circ$ |
| V | 813.03 \AA^3 | 795.80 \AA^3 |
| $d(\text{calc})$ | 1.868 g cm^{-3} | 1.909 g cm^{-3} |

Although parameters could be inferred from symmetry and packing arguments, the structure was determined from a Patterson synthesis and successive Fourier syntheses phased on least-squares refined positional and isotropic thermal parameters. The function

$w(F_o - F_c)^2$ was minimized with $w = 1/\sigma^2$ and with structure factors calculated using scattering factors taken from Tables 3.3.1A and 3.3.1B of *International Tables for X-ray Crystallography* (1962) and from Stewart, Davidson & Simpson (1965) for hydrogen. With two dimer units per cell in space group $C2/m$ (initially assumed and verified by agreement in the final refinement), the linear chain (Fig. 2) and the pyrazine molecule are situated on mirror planes with inversion centers midway between the Cu-Cu linkage and in the center of the pyrazine molecule. Thus, Cu, N and two C of the pyrazine molecule [designated C(1) and C(2) in Tables 2 and 3] occupy $(x, 0, z)$ sites while the acetate ions [O(1), O(2), C(3) and methyl C(4) in general positions] are related to each other by the mirror and inversion center. Hydrogen atoms were obtained on a Fourier synthesis calculated with structure factors from anisotropic thermal parameters, least-squares refined model; these were also assigned a nonvarying isotropic parameter and the positions together with anisotropic parameters for the remaining atoms were subjected to further least-squares refinement. The residuals $R = \sum ||F_o| - |F_c|| / \sum |F_o|$ were 0.048 and 0.055 for the 300 and 100K data, respectively.* Table 2 lists the positional and thermal parameters and Table 3 gives the interatomic separations and angles. The X-RAY system (Stewart, 1971) was used for calculations.

The e.p.r. spectra were obtained with a standard Varian Q -band bridge, operating around 35GHz, with 100 kHz modulation and detection. The Fieldial (registered trademark of Varian Ass.) magnetic-field sweep and readout were calibrated with a Harvey-Wells gaussmeter, which had proton and ^7Li resonances at the appropriate fields. The n.m.r. frequencies were read with a Hewlett-Packard frequency meter and the microwave frequencies were read from the bridge

* A list of structure factors has been deposited with the British Library Lending Division as Supplementary Publication No. SUP 30749 (8 pp.). Copies may be obtained through The Executive Secretary, International Union of Crystallography, 13 White Friars, Chester CH1 1NZ, England.

Table 2. Positional and thermal parameters for $PzCuAc$ at 300K (upper values) and 100K (lower values)

U_{ij} are of the form $\exp(-2\pi^2 \sum U_{ij} h_i h_j a_i^* a_j^*)$ in units 10^{-2} \AA^2 .

| | x | y | z | U_{11} | U_{22} | U_{33} | U_{12} | U_{13} | U_{23} |
|------|-------------|------------|-------------|----------|----------|----------|----------|-----------|----------|
| Cu | 0.1381 (1) | 0 | 0.1262 (1) | 1.72 (4) | 2.63 (5) | 2.11 (4) | 0 | -0.15 (3) | 0 |
| | 0.1380 (1) | 0 | 0.1261 (1) | 1.02 (3) | 1.12 (3) | 0.71 (3) | 0 | 0.00 (2) | 0 |
| N | 0.3602 (9) | 0 | 0.3515 (9) | 2.4 (3) | 5.0 (4) | 2.4 (3) | 0 | -0.4 (3) | 0 |
| | 0.3613 (7) | 0 | 0.3500 (7) | 1.3 (2) | 2.0 (3) | 1.5 (2) | 0 | -0.1 (2) | 0 |
| C(1) | 0.5211 (11) | 0 | 0.3253 (12) | 2.2 (4) | 7.9 (7) | 2.7 (4) | 0 | 0.1 (3) | 0 |
| | 0.5233 (9) | 0 | 0.3249 (10) | 2.4 (3) | 3.6 (4) | 1.7 (3) | 0 | 0.5 (3) | 0 |
| C(2) | 0.6606 (11) | 0 | 0.4727 (12) | 2.3 (4) | 8.3 (8) | 2.6 (4) | 0 | 0.3 (3) | 0 |
| | 0.6643 (9) | 0 | 0.4732 (9) | 1.7 (3) | 3.9 (4) | 1.1 (3) | 0 | 0.2 (2) | 0 |
| C(3) | 0.1265 (8) | 0.1271 (4) | 0.8263 (8) | 3.6 (3) | 3.1 (3) | 3.4 (3) | -0.6 (2) | 1.1 (2) | 0.0 (2) |
| | 0.1302 (6) | 0.1288 (3) | 0.8255 (6) | 2.3 (2) | 1.6 (2) | 1.3 (2) | -0.1 (2) | 0.6 (2) | 0.0 (2) |
| C(4) | 0.1977 (12) | 0.2060 (6) | 0.7272 (12) | 6.7 (5) | 5.2 (5) | 6.2 (5) | -3.1 (4) | 1.8 (4) | 1.3 (4) |
| | 0.2031 (7) | 0.2080 (4) | 0.7264 (7) | 3.3 (3) | 2.9 (3) | 2.3 (2) | -1.0 (2) | 0.7 (2) | 0.5 (2) |
| O(1) | -0.0198 (6) | 0.0984 (3) | 0.7581 (6) | 3.9 (2) | 4.4 (3) | 3.7 (2) | -0.6 (2) | 0.2 (2) | 1.2 (2) |
| | -0.0181 (4) | 0.0986 (2) | 0.7569 (4) | 2.0 (2) | 2.0 (2) | 1.8 (2) | -0.4 (1) | 0.2 (1) | 0.5 (1) |
| O(2) | 0.2186 (6) | 0.0967 (4) | -0.0272 (6) | 3.8 (2) | 4.8 (3) | 3.8 (2) | -1.1 (2) | 0.1 (2) | 0.8 (2) |
| | 0.2232 (4) | 0.0974 (2) | -0.0273 (4) | 2.0 (2) | 2.2 (2) | 1.6 (2) | -0.6 (1) | 0.2 (1) | 0.3 (1) |

Table 2 (cont.)

| | <i>x</i> | <i>y</i> | <i>z</i> | <i>U</i> |
|------|----------|-----------|----------|----------|
| H(1) | 0.52 (2) | 0 | 0.19 (2) | 3.8 |
| | 0.55 (2) | 0 | 0.20 (2) | 3.8 |
| H(2) | 0.77 (2) | 0 | 0.44 (2) | 3.8 |
| | 0.78 (2) | 0 | 0.46 (2) | 3.8 |
| H(3) | 0.13 (1) | 0.256 (7) | 0.73 (1) | 3.8 |
| | 0.14 (1) | 0.254 (7) | 0.81 (1) | 3.8 |
| H(4) | 0.33 (1) | 0.194 (7) | 0.75 (1) | 3.8 |
| | 0.32 (1) | 0.202 (6) | 0.76 (1) | 3.8 |
| H(5) | 0.23 (1) | 0.161 (6) | 0.56 (1) | 3.8 |
| | 0.17 (1) | 0.197 (6) | 0.60 (1) | 3.8 |

Table 3. Interatomic separations and angles for PzCuAc

| | 300 K | 100 K |
|----------------|-------------|-------------|
| Cu—Cu | 2.583 (1) Å | 2.576 (1) Å |
| Cu—O(1) | 1.968 (5) | 1.963 (4) |
| Cu—O(2) | 1.960 (5) | 1.966 (4) |
| Cu—N | 2.171 (6) | 2.167 (5) |
| O(1)—C(3) | 1.244 (7) | 1.258 (5) |
| O(2)—C(3) | 1.253 (7) | 1.260 (5) |
| C(3)—C(4) | 1.505 (12) | 1.500 (8) |
| N—C(1) | 1.332 (12) | 1.330 (10) |
| N—C(2) | 1.329 (12) | 1.344 (9) |
| C(1)—C(2) | 1.390 (11) | 1.399 (9) |
| O(1)—O(1) | 2.797 (7) | 2.766 (5) |
| O(2)—O(2') | 2.748 (7) | 2.733 (5) |
| O(1)—O(2) | 2.217 (6) | 2.232 (4) |
| O(1)—O(2') | 2.757 (7) | 2.785 (5) |
| C(1)—H(1) | 1.00 (13) | 0.99 (14) |
| C(2)—H(2) | 0.90 (14) | 0.97 (13) |
| C(4)—H(3) | 0.90 (10) | 1.03 (10) |
| C(4)—H(4) | 1.05 (9) | 0.90 (9) |
| C(4)—H(5) | 1.45 (9) | 0.93 (8) |
| O(1)—Cu—O(1) | 90.6 (2)° | 89.6 (1)° |
| O(2)—Cu—O(2) | 89.0 (2) | 88.1 (1) |
| O(1)—Cu—O(2) | 89.2 (2) | 90.3 (1) |
| N—Cu—O(1) | 93.5 (2) | 93.7 (1) |
| N—Cu—O(2) | 97.2 (2) | 96.4 (1) |
| Cu—Cu—N | 176.4 (2) | 176.8 (2) |
| Cu—N—N | 178.4 (4) | 177.4 (3) |
| Cu—O(1)—C(3) | 123.4 (4) | 123.7 (3) |
| Cu—O(2)—C(3) | 122.0 (4) | 121.4 (3) |
| O(1)—C(3)—O(2) | 125.3 (6) | 124.8 (4) |
| O(1)—C(3)—C(4) | 117.6 (6) | 118.2 (4) |
| O(2)—C(3)—C(4) | 117.2 (6) | 117.0 (4) |
| Cu—N—C(1) | 123.7 (6) | 124.4 (5) |
| Cu—N—C(2) | 119.9 (6) | 118.3 (4) |
| C(1)—N—C(2) | 116.3 (7) | 117.3 (5) |
| N—C(1)—C(2) | 122.3 (9) | 122.7 (7) |
| N—C(2)—C(1) | 121.3 (8) | 120.0 (6) |

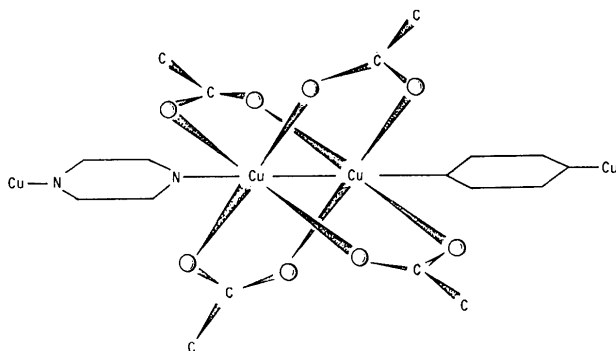


Fig. 2. Sketch of linear chains in PzCuAc.

frequency meter and cross-checked with the DPPH e.p.r. transition. The centers of the rather broad e.p.r. transitions in PzCuAc were taken to be where the first derivative of the absorption spectrum crosses the baseline and also half-way between the symmetrical peaks of the first derivative spectra. The principal error in the values of D and g comes from the reproducibility of the position of the center of the line from crystal to crystal, rather than the precision of the magnetic field and frequency. As expected, the weak $\Delta m = 2$ transition was observed with H_0 perpendicular to the c axis at 5800 ± 10 G (for $h\nu_0 = 35000$ MHz).

The transition fields, corrected to 35 GHz are given in Table 4 for the field parallel and perpendicular to the chain axis. The maximum and minimum splittings in the perpendicular direction are given and were 90° apart, which defined g_x and g_y .

Table 4. E.p.r. transitions

| Transitions at 35000 MHz in G (error is ± 10) | | |
|--|-------|-------|
| | 300 K | 120 K |
| \perp to needle | | |
| Max. | 13744 | 13731 |
| | 10205 | 10266 |
| Min. | 13739 | 13711 |
| | 10240 | 10274 |
| \parallel to needle | 13611 | 13630 |
| | 7621 | 7650 |

Structural results

(a) 300K structure

The Cu—Cu separation is among the shortest found in known dimer-type compounds. The present room-temperature value of 2.583 Å may be compared with values determined in HyCuAc and in two modifications of pyridine (Py) complexes (Table 5). The influence of the ligands (N from pyrazine or pyridine and O from water) does not appear to establish a trend, primarily because of the large differences in the pyridine compounds. The 2.610 Å Cu—Cu separation in copper succinate dihydrate (O'Connor & Maslen, 1966) is in agreement with values for HyCuAc. Brown & Chidambaram (1973) attribute the shorter Cu—Cu separation in HyCuAc as strengthening the argument for direct electronic interaction between the two copper atoms in the unit; however, our separation is even shorter. They compared their separation to that in metallic copper, in which the separation is 2.556 Å. With different electronic structures, we feel such comparisons may not be valid.

A comparison of the Cu—O(acetate) separations proves interesting; however, unfortunately, the values of the standard deviations are sufficiently large that one can only speculate on effects present. The longer sets of Cu—O separations in HyCuAc are influenced by hydrogen bonding and suggest a charge transfer away from the oxygen towards the hydrogen ion, the reduced charge on the oxygen forming a weaker bond to the Cu^{2+} ion. This in turn appears to decrease the reso-

nance within the acetate group, resulting in a trend of slightly longer C–O bonds in HyCuAc compared with PzCuAc.

The remaining separations are as expected, with small differences explained by packing requirements. In Fig. 3, the small departure of the chains from a straight line is indicated. A slight zigzag is found so that the kink at the copper (*i.e.* the Cu–Cu–N angle) is such as to tip the nitrogen away from one side and towards the other side of the rectangular base (formed by four oxygen atoms) about the copper ion. This results in N(Pz)–O(Ac) and C(Pz)–O(Ac) separations differing by about 0.1 Å. The O–O separations themselves are influenced by this zigzag, being further apart (2.797 Å) where the nitrogen atom is inserted compared with the other pair (2.748 Å). The copper ion is situated slightly above (0.28 Å) the plane through the four oxygen atoms; this is generally the case in such dimer compounds.

The anisotropic thermal parameters of the pyrazine molecule suggest a rocking motion pivoted about the nitrogen atoms. The thermal parameters for the copper oxygen framework do not appear to depart from expected results.

(b) 100K structure

The Cu–Cu separation of 2.576 (1) Å is significantly shorter than the room-temperature value. The remainder of the separations within the dimer are not significantly different from those at room temperature. The exceptions result from the contraction along the *b* axis of the structure; hence, the O–O separations across the mirror reduce from 2.797 to 2.766 Å and from 2.748 to 2.733 Å while the remaining O–O separation nearly parallel to the mirror increases from 2.757 to 2.785 Å. These separations (and the corresponding angles) do not change the basic arrangement of the chain, *i.e.* it remains zigzagged; the copper ion remains above (0.26 Å) the plane through the oxygen atoms. The volume is decreased significantly.

The remaining significant differences between the

300 and 100K structures concern the thermal parameters. Overall these are reduced by $\frac{1}{3}$ to $\frac{1}{2}$ of their room-temperature values. In particular the values perpendicular to the mirror for the carbon atoms of the pyrazine molecule are reduced the most, suggesting that the rocking motion probably is real rather than the presence of a slight disordering in the positions of the carbon atoms due to close contacts resulting from the zigzag nature of the linear chains.

(c) Exchange-striction

The small difference in the Cu–Cu separation [2.583 (1) *vs.* 2.576 (1) Å] is smaller by almost an order of magnitude than the expected difference of 0.04 Å, for an exchange striction of 0.12 Å; the presumed change in the singlet–triplet separation is 0.02 Å if the entire Cu–Cu change is due to the 37% change in the triplet concentration. The observed difference is that typically found in normal thermal expansion of linear chain compounds [the Co–Co separations in CoCl₂·2H₂O at 300 and 5K are 3.569 and 3.564 Å, respectively (Morosin, 1966)].

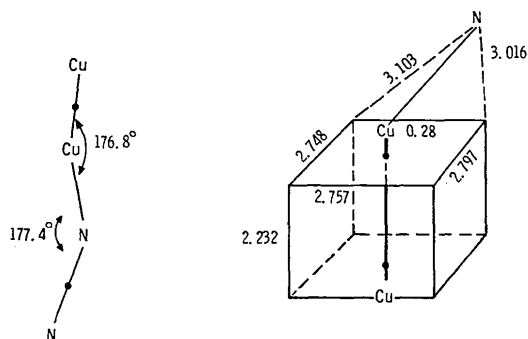


Fig. 3. Sketch of details of the chain and copper environment. The Cu–Cu–N(C₄H₄)N–Cu chains are not perfectly linear, but form a slight zigzag. The copper ion sits above the plane through the oxygen atoms and the kink in the chain (greatly exaggerated in the figure) results in closer and more distant oxygen neighbors for the nitrogen atom.

Table 5. Selected dimer separations (Å)

| | This study | HyCuAc* | HyCuAc† | α -PyCuAc‡ | β -PyCuAc§ |
|-----------------|------------|-----------|-----------|-------------------|------------------|
| Cu–Cu | 2.583 (1) | 2.616 (1) | 2.614 (2) | 2.645 (3) | 2.630 (3) |
| Cu–X (ligand) | 2.171 (6) | 2.156 (4) | 2.161 (2) | 2.186 (8) | 2.122 (9) |
| | | | | | 2.129 (11) |
| Cu–O (acetates) | 1.968 (5) | 1.986 (3) | 1.990 (1) | 1.978 (8) | 1.985 (10) |
| | 1.960 (5) | 1.994 (3) | 1.992 (1) | 1.965 (7) | 1.973 (10) |
| | | 1.945 (4) | 1.942 (2) | 1.948 (8) | 1.985 (10) |
| | | 1.950 (3) | 1.952 (2) | 1.928 (8) | 1.982 (10) |
| C–O (acetate) | 1.244 (7) | 1.251 (6) | 1.257 (2) | 1.248 (20) | 1.247 (16) |
| | 1.253 (7) | 1.268 (6) | 1.261 (2) | 1.236 (19) | 1.247 (15) |
| | | 1.274 (7) | 1.259 (2) | 1.250 (22) | 1.231 (21) |
| | | 1.248 (6) | 1.261 (2) | 1.250 (23) | 1.231 (21) |
| C–C (methyl) | 1.505 (12) | 1.495 (5) | 1.500 (2) | 1.525 (25) | 1.467 (22) |
| | | 1.506 (7) | 1.502 (2) | 1.549 (27) | 1.540 (26) |

* Recent X-ray redetermination by de Meester, Fletcher & Skapski (1973).

† Recent neutron diffraction study by Brown & Chidambaram (1973).

‡ Orthorhombic form (Hanic, Štempelová & Hanicová, 1964).

§ Monoclinic form (Barclay & Kennard, 1961).

If we now consider the effect of thermal vibrations on the problem and follow a treatment similar to Leipoldt & Coppens (1973), we note that the acoustic vibrations of the lattice will be superimposed on any real difference in the time-averaged structure of the diffraction experiment. The random distribution of triplet fluctuations seen in e.p.r. indicated that the room-temperature structure could be considered to be a superposition of the two states, each with slightly different equilibrium Cu–Cu separations. An examination of the average values of the U_{ii} and their ratios (Table 6) suggests that there are no anomalous values with respect to the copper environment. In particular the ratios of the room-temperature to low-temperature thermal values are nearly identical.

Table 6. Average U_{ij} values at 300 and 100K

| | 300 K | 100 K | Ratio U_{300}/U_{100} |
|----|--------|--------|-------------------------|
| Cu | 0.0215 | 0.0107 | 2.01 |
| O | 0.407 | 0.0197 | 2.07 |
| N | 0.0324 | 0.0160 | 2.02 |

Pursuing the problem further, the superposition of two Gaussian distributions (defining the thermal motion) of equal occupancy at a distance of $2x_0$ gives a (non-Gaussian) distribution with root-mean-square displacements as

$$(U_{ij})_{\text{new}} = (U_{ij})_{\text{old}} + x_0^2.$$

In our case, we should have attained only $\sim 40\%$ rather than 50% in the triplet state; however, it is easily seen that a difference of 0.12 \AA in the Cu–Cu separation would appear as an apparent increase in the corresponding thermal parameter of 0.0144 \AA^2 . This is sufficiently large, that the ratios shown on Table 6 should easily indicate such a change. However, an apparent increase in the copper thermal parameter of one order of magnitude less (0.001 \AA^2) which corresponds to a smaller value for the difference of the Cu–Cu separation (0.03 \AA) would be within the error limits of this problem. In this analysis we have considered an average or isotropic thermal parameter; however, a similar conclusion is obtained when values along the Cu–Cu separation are considered. Furthermore, since no anomalies were found in the difference Fourier synthesis calculated when the refinement was completed, one can conclude that the presence of disorder resulting from the population of two states requires that such states probably differ by an amount significantly smaller than 0.03 \AA .

E.p.r. results

(a) Magnetic parameters

The CuAc dimer in PzCuAc was described in VSS by the triplet spin Hamiltonian (Bleaney & Bowers, 1952)

$$H_T = \mu_B \mathbf{S} \cdot \mathbf{g} \cdot \mathbf{H}_0 + DS_z^2 + E(S_x^2 - S_y^2) \quad (1)$$

where \mathbf{H}_0 is the applied field, μ_B is the Bohr magneton, and $\mathbf{S} = 1$. Both the \mathbf{g} tensor and fine-structure tensor have principal axes with \hat{z} defined to be along the Cu–Cu axis (Fig. 2). The Q -band redetermination of the magnetic parameters is shown in Table 7 and provides greater accuracy than at X -band. This occurs primarily because $\mathbf{g} \mu_B \mathbf{H}_0$ is now larger than D and thus a typical two-line triplet spectrum is seen at Q -band for \mathbf{H}_0 either parallel or perpendicular to the Cu–Cu axis. The almost complete isotropy in the $\hat{x}\hat{y}$ plane establishes that $g_{\hat{x}} \simeq g_{\hat{y}}$ and that $E \simeq 0$. The present bounds on $|g_{\hat{x}} - g_{\hat{y}}|$ and on E are an order of magnitude smaller than the X -band values in VSS. Comparison with other substituted CuAc complexes (Kokoszka & Gordon) shows that PzCuAc provides by far the most nearly axially symmetric \mathbf{g} tensor and the smallest E value. Thus the D_{4h} symmetry for the dimer that is usually adopted for theoretical analyses (Bleaney & Bowers, 1952; Hansen & Ballhausen, 1965) is an excellent approximation here. It should be noted that, with $E = 0$ and $\mathbf{g} \mu_B \mathbf{H}_0 > D$, the values of g_{\parallel} and D_{\parallel} and of g_{\perp} and D_{\perp} can both be determined from a *single* e.p.r. spectrum with \mathbf{H}_0 parallel and perpendicular to \hat{z} , respectively. This feature of the high-field triplet spectrum is exploited below to separate spin-orbit and dipolar contributions to D .

Table 7. Magnetic parameters of PzCuAc

| | 300 K | 120 K |
|--|---------------------|---------------------|
| g_{\parallel} | 2.355 ± 0.002 | 2.350 ± 0.002 |
| g_{\perp} | 2.066 ± 0.002 | 2.064 ± 0.002 |
| $ g_{\hat{x}} - g_{\hat{y}} $ | 0.002 | 0.0004 |
| $D(\mathbf{H}_0 \parallel \hat{z}) (\text{cm}^{-1})$ | 0.329 ± 0.001 | 0.328 ± 0.001 |
| $(\mathbf{H}_0 \perp \hat{z}) (\text{cm}^{-1})$ | 0.335 ± 0.001 | 0.329 ± 0.001 |
| $E (\text{cm}^{-1})$ | 0.0010 ± 0.0002 | 0.0005 ± 0.0002 |

With $E = 0$ the Q -band spectrum for $\mathbf{H}_0 \parallel \hat{z}$ contains lines at $g_{\parallel} \mu_B H_0 \pm D$, as indicated in Table 4. Corrections due to $E \neq 0$ go as $E^2 / (g_{\parallel} \mu_B H_0)^2$ and are entirely negligible for $E < 80\text{G}$. The corresponding $\Delta m = 1$ transitions for $\mathbf{H}_0 \perp \hat{z}$ also follow standard analysis (Carlington & McLachlan, 1967), but care has been taken to retain the lowest-order corrections in $(D/g_{\perp} \mu_B H_0)^2$. Furthermore, the small variation in the splitting of less than 60G out of 3500G as \mathbf{H}_0 is rotated in the $\hat{x}\hat{y}$ plane provides the value of E in Table 7 and requires an average of $\mathbf{H}_0 \parallel \hat{x}$ and $\mathbf{H}_0 \parallel \hat{y}$. If we let H_1, H_2 be the two transitions for the maximum splitting ($\mathbf{H}_0 \parallel \hat{x}$) and H_3, H_4 be the transitions for the minimum splitting ($\mathbf{H}_0 \parallel \hat{y}$), then for $\mathbf{H}_0 \perp \hat{z}$ we have

$$D = \hbar \omega_0 \frac{1}{2} \left(\frac{H_1^2 - H_2^2}{H_1^2 + H_2^2} + \frac{H_3^2 - H_4^2}{H_3^2 + H_4^2} \right) \quad (2)$$

where $\hbar \omega_0$ is the microwave frequency and $H_1 > H_2$, $H_3 > H_4$ and corrections are of order $E^2 / (\hbar \omega_0)^2$ and thus negligible. Equation (2) reduces, in the high-field limit of $H_2 \gg H_1 - H_2$, to transitions at $g_{\perp} \mu_B H_0 \pm \frac{1}{2} D$, but this limit does not hold at Q -band, since $|H_1 - H_2| \sim \frac{1}{3} H_0$. The value of g_{\perp} is then

$$g_{\perp} = \frac{2\hbar\omega_0}{\mu_B(H_1 + H_2)} \left\{ 1 - \frac{1}{2} \left(\frac{D}{g_{\perp}\mu_B(H_1 + H_2)} \right)^2 \right\}, \quad (3)$$

where the correction term is about $\frac{1}{2}\%$ and there is a negligible difference between using the fields for the maximum or minimum splitting in the $\hat{x}\hat{y}$ plane.

The difference in the values of D based on spectra with \mathbf{H}_0 parallel and perpendicular to \hat{z} will now be related to the dipolar interaction between the two unpaired electrons in the triplet state. The principal temperature dependence observed between 300 and 120K and summarized in Table 4 is a shift in the low-field line of the spectra with $\mathbf{H}_0 \perp \hat{z}$. The anisotropy in the $\hat{x}\hat{y}$ plane is thus lower at 120K, with E more nearly vanishing; but the g values also change slightly, as otherwise both lines of the perpendicular spectrum would shift on reducing E . These small changes, which were reproducibly observed on several carefully oriented single crystals, are close to the $\pm 10G$ experimental uncertainty and will not be explored in detail. The principal conclusion from the more accurate Q -band parameters summarized in Table 7 is that there is very little change, if any, in the fine-structure splittings observed at 300 and 120K. We now turn to the dependence of D on the Cu-Cu separation.

(b) Cu-Cu separation

Bleaney (1953) pointed out that the spin-orbit contribution of D dominates the magnetic dipole contribution and that the two terms have opposite signs. The Q -band data confirm both assertions and provide the first separation of D into its spin-orbit and dipolar contributions. Since both contributions are directly related to the Cu-Cu separation in the triplet state, the single-crystal Q -band data at 120 and 300K complement the X-ray structural search for exchange striction.

The idealized D_{4h} symmetry generally adopted for binuclear copper acetate complexes is, as summarized in Table 7, very nearly achieved in PzCuAc, whose g anisotropy in the $\hat{x}\hat{y}$ plane and E value are an order of magnitude smaller than in HyCuAc (Kokoszka & Gordon, 1969). The spin-orbit contribution (Bleaney & Bowers, 1952) is

$$D_{so} = -\frac{1}{8}\{J_1(g_{\parallel} - 2)^2/4 - J_2(g_{\perp} - 2)^2\}. \quad (4)$$

Here J_1 and J_2 are exchange interactions in electronically excited states of the dimer. If both are antiferromagnetic (negative in Bleaney's notation) and comparable to the ground-state exchange J , then D_{so} values of $\sim 1 \text{ cm}^{-1}$ are obtained, in rough agreement with experiment. Smaller exchange is expected in the excited states, since a charge-transfer mechanism available for the ground state becomes inoperative (Hansen & Ballhausen, 1965). While the magnitude of J_1 and J_2 are not known, they should depend sensitively on the Cu-Cu separation in the triplet state and thus provide a qualitative e.p.r. check on the Cu-Cu separation.

The familiar dipolar contribution (Carrington & McLachlan, 1967) to D is, for an isotropic g value,

$$D_d = \frac{3}{4}g^2\mu_B^2 \left\langle \frac{r_{12}^2 - 3z_{12}^2}{r_{12}^5} \right\rangle \quad (5)$$

where r_{12} is the distance between the two unpaired electrons and the expectation value is for the triplet state, with each electron in an approximately $3d_{x^2-y^2}$ orbital. The point-dipole limit, with $r_{12} = \bar{R}$, shows that D_d is negative, and thus both opposes D_{so} and has a smaller magnitude. The anisotropy of the g tensor in PzCuAc provides the basis for separating D_d and D_{so} . In a strong field, with $H_0 \gg D$, the magnetic moments are quantized along \mathbf{H}_0 and, for $\mathbf{H}_0 \parallel \hat{z}$, have an effective value of $g_{\parallel}\mu_B$ while, for $\mathbf{H}_0 \perp \hat{z}$, they are $g_{\perp}\mu_B$. At Q -band we have $g_{\perp}\mu_B H_0 \gtrsim 3D$ and, except for a correction of about 2%, the effective magnetic moments are $g_{\perp}\mu_B$ and $g_{\parallel}\mu_B$.

Thus slightly different values for $D = D_{so} + D_d$ should be observed when the applied field is parallel or perpendicular to the \hat{z} axis, as indeed are found. The difference is

$$D_{\perp} - D_{\parallel} = \frac{3}{4}(g_{\parallel}^2 - g_{\perp}^2)\mu_B^2 \left\langle \frac{3z_{12}^2 - r_{12}^2}{r_{12}^5} \right\rangle \quad (6)$$

if D_d has the opposite sign from D_{so} , as expected for $3z_{12}^2 > r_{12}^2$. The high-field single-crystal e.p.r. thus provides, through the anisotropy of the g tensor, a direct experimental determination of the function

$$F(r_{12}; \bar{R}) = \frac{1}{2} \left\langle \frac{3z_{12}^2 - r_{12}^2}{r_{12}^5} \right\rangle. \quad (7)$$

$F(r_{12}; \bar{R})$ reduces to \bar{R}^{-3} for point dipoles at the two copper nuclei at 0,0,0 and 0,0, \bar{R} , respectively. The average value observed, using both the maximum and minimum splittings on the $\hat{x}\hat{y}$ plane to eliminate any E dependence, is $F(r_{12}; \bar{R}) \sim 4 \pm 3 \times 10^{21} \text{ cm}^{-3}$, which is about 10% of value of \bar{R}^{-3} at the observed Cu-Cu separation of 2.58 Å. The small value of $F(r_{12}; \bar{R})$ can be related to the delocalization (finite extent) of the $3d_{x^2-y^2}$ orbitals in which, to a good first approximation, the unpaired electrons are found. The identity

$$F(r_{12}; \bar{R}) = \frac{1}{2} \frac{d^2}{d\bar{R}^2} \left\langle \frac{1}{r_{12}} \right\rangle \quad (8)$$

relates $F(r_{12}; \bar{R})$ to the curvature of the Coulomb integral, whose analytic form is known (Kotani, 1955; the $D_{3\zeta_3\zeta_3\zeta_3\zeta_3}$ integral on p. 104 corresponds to $\langle 1/r_{12} \rangle$). At the experimental Cu-Cu separation of 2.58 Å, or about ten units of $3a_0/Z_{\text{eff}}$ in terms of the effective charge $Z_{\text{eff}} \approx 6$, $F(r_{12}; \bar{R})$ is decreased by a factor of 3 and, indeed, becomes negative for small \bar{R} . Since the $3d_{x^2-y^2}$ orbitals are probably further delocalized by the ligand charges, the reduced magnitude of the dipolar interaction is not surprising. What is unexpected, however, is the very gentle distance dependence of $F(r_{12}; \bar{R})$ for $3d_{x^2-y^2}$ orbitals. It is practically flat in the 5-10 units of $3a_0/Z_{\text{eff}}$ in contrast to the \bar{R}^{-3} dependence expected for point dipoles.

The dipolar contribution to D is found by combining (5) and (7) to be

$$D_d = -\frac{3}{2}g_{\parallel}^2\mu_B^2F(r_{12}; \bar{R}) \quad (9)$$

for $\mathbf{H}_0 \parallel \hat{z}$, with a corresponding expression for $\mathbf{H}_0 \perp \hat{z}$ using g_{\perp}^2 . Thus the dipolar contribution is small, about 5–10% of D , and in fact has the opposite sign from D_{so} . Furthermore, it is not sensitive to small changes in \bar{R} around the equilibrium separation, as would occur in either thermal contraction or Cu–Cu vibrations.

The small e.p.r. changes observed between 300 and 120K occur primarily in the low-field line of the perpendicular spectrum and are therefore most likely to be associated with very small changes in E and in $|g_{\hat{x}} - g_{\hat{y}}|$. This is consistent with the observed contraction along the b axis and the changed O–Cu–O angles listed in Table 3, although it is speculative to try to interpret the net effect of such small changes. The point is that no significant D -value changes were observed between 300 and 120K and that at most very small corrections could come from D_d . Thus we do not find changes in the excited state exchange interactions, J_1 or J_2 in equation (2). Since the accuracy is ± 10 G in splittings of 3500G for $\mathbf{H}_0 \perp \hat{z}$ and almost 6000G for $\mathbf{H}_0 \parallel \hat{z}$, even a 1% change in J_1 and J_2 with temperature would be readily detected, given the insensitivity of D_d to small changes in \bar{R} . Furthermore exchange or superexchange interactions are often quite sensitive to changes in \bar{R} (Morosin, 1970). The e.p.r. data indicate that there is no detectable change in the Cu–Cu separation of the triplet state between 300 and 120K.

Discussion

The absence of detectable triplet motion in PzCuAc in spite of an interdimer exchange $J' \sim 1100$ G, which is far greater than the resolved low-temperature hyperfine structure, was taken in VSS to be evidence for exchange striction. This interpretation still provides the simplest explanation for the e.p.r. and is further supported by the very small temperature dependence of the fine-structure splittings reported here. The structural data, by contrast, can be interpreted by either thermal expansion or by a small exchange striction of < 0.03 Å, as discussed in section (c) above, but not by the striction of 0.12 Å suggested in VSS. The estimate of 0.12 Å was obtained by taking each Cu_2Ac_4 unit as a single harmonic oscillator, with the same energy $\hbar\omega_0 \sim 100$ cm^{-1} in both singlet and triplet state and a mass of $2\text{Cu} \sim 130$ a.u. The Frank–Condon overlap $\Gamma = \langle \varphi_s | \varphi_t \rangle$ is then easily computed at 0K and reduces the triplet transfer integral (or bandwidth) by

$$\left\langle S\varphi_s T\varphi_t \left| \frac{J'}{4} S_1 \cdot S_2 \right| T\varphi_t S\varphi_s \right\rangle = \frac{J'}{4} \Gamma^2. \quad (10)$$

Here S and T are the singlet and triplet (with $S_z = 0$) functions and S_1, S_2 are the total electronic spins of the

adjacent dimers. Equation (10) describes the motion of a triplet from one dimer to the next when the accompanying changes in the lattice coordinates are included, and is the basis for triplet-exciton motion in organic free-radical solids (Nordio, Soos & McConnell, 1966).

Each copper acetate dimer has, of course, many additional vibrational degrees of freedom and the product of all the displaced normal oscillators should be used in (10). The generalization to different normal frequencies in the triplet and singlet state and to a thermal average over the nuclear vibrations presents no difficulties, but yields additional unknown parameters. The low-temperature structural changes, aside possibly from the Cu–Cu separation, are not easily correlated with a triplet or singlet state, however, and are probably just thermal contractions arising primarily from the decrease of the b axis. Small changes in force constants and low temperatures (compared to vibrations of a dimer) do not seriously alter the 0K result. We therefore do not believe that the additional complexities of many vibrational degrees of freedom, of different force constants, and of finite temperature can be used to change the estimate given in VSS.

The difficulty lies instead in the frequently used approximation of taking a bandwidth, as in equation (10), and simply dividing by \hbar to obtain a hopping rate. Such estimates have been used for charge carriers, for singlet or triplet excited states, and for spin excitations, with the associated lattice distortions yielding polarons of various types (Austin & Mott, 1969; Emin, 1974). It turns out that the estimates based on (bandwidth)/ \hbar are upper bounds on the hopping rate and are often far too large (Emin, 1974). For example, it is natural to treat the Cu–Cu vibrations in the PzCuAc chains as optical modes. An exchange striction of $\delta = 0.02$ Å in the Cu–Cu separation yields a polaron binding energy of $E_b = m\omega_0^2\delta^2/2 \simeq \sim 8$ cm^{-1} for $m \simeq 130$ a.u. and $\hbar\omega_0 \sim 100$ cm^{-1} . An even smaller value of E_b occurs if part of the observed contraction in the Cu–Cu separation is attributed to thermal effects instead of, as above, entirely to exchange striction. The weak coupling limit $E_b \ll \hbar\omega_0$ then applies for these spin polarons (Emin, 1974, Appendix E). Without going into the different temperature regimes, we see that the hopping rate is reduced from the bandwidth estimate given by (10), by factors of both $(J'/\hbar\omega_0)$ and $(E_b/\hbar\omega_0)$. The former is 10^{-3} , the latter 10^{-1} in PzCuAc. The rate of motion is slow enough to allow, even for $J' \sim 1100$ G, resolvable hyperfine even with negligible exchange striction.

The resolved low-temperature hyperfine in PzCuAc proves that the triplet state is localized on a dimer. Thus localization is established, in contrast to other types of polarons in which the question of localization is difficult to answer. While $J' \sim 1100$ G (or ~ 0.1 cm^{-1}) is large compared with magnetic quantities, it is negligible compared with vibrational frequencies. Thus the triplet state in PzCuAc remains on a dimer long enough to allow for nuclear distortions and the formation of a

spin polaron. The binding energy and the change in the Cu–Cu separation are both quite small, since so little electronic energy (of order J) can be gained by distorting the lattice. The distinction between spin polarons, which we believe provide the most convincing explanation of the magnetic properties, and thermal contraction then cannot be made from structural data alone. The desirability of a linear chain of copper acetate dimers with a larger value of J' , even if only by an order of magnitude, is evident both for establishing exchange striction on a structural basis and for observing triplet spin excitons in an inorganic system.

References

- AUSTIN, I. G. & MOTT, N. F. (1969). *Advanc. Phys.* **18**, 41–102.
- BARCLAY, G. A. & KENNARD, C. H. L. (1961). *J. Chem. Soc.* pp. 5244–5251.
- BARTKOWSKI, R. R. & MOROSIN, B. (1972). *Phys. Rev.* **B6**, 4209–4212.
- BLEANEY, B. (1953). *Rev. Mod. Phys.* **25**, 161–162.
- BLEANEY, B. & BOWERS, K. D. (1952). *Proc. Roy. Soc. A* **214**, 451–465.
- BROWN, G. M. & CHIDAMBARAM, R. (1973). *Acta Cryst.* **B29**, 2393–2403.
- CARRINGTON, A. & McLACHLAN, A. D. (1967). *Introduction to Magnetic Resonance*, chap. 8. New York: Harper & Row.
- EMIN, D. (1974). *Advanc. Phys.* To be published.
- HANIC, F., ŠTEMPELOVÁ, D. & HANICOVÁ, K. (1964). *Acta Cryst.* **17**, 633–639.
- HANSEN, A. E. & BALLHAUSEN, C. J. (1965). *Trans. Faraday Soc.* **61**, 631–639.
- International Tables for X-ray Crystallography* (1962). Vol. III. Birmingham: Kynoch Press.
- KOKOSZKA, G. F. & GORDON, G. (1969). *Transition Metal Chem.* **5**, 181–277; see also HATFIELD, W. E. & WHYMAN, R. (1969). *Transition Metal Chem.* **5**, 47–179.
- KOTANI, M. (1955). *Table of Molecular Integrals*, p. 104. Tokyo: Maruzen.
- LEIPOLDT, J. & COPPENS, P. (1973). *Inorg. Chem.* pp. 2269–2274.
- MARTIN, R. L. (1966). *Inorg. Chem.* **5**, 2065–2067.
- MARTIN, R. L. (1968). *New Pathways in Inorganic Chemistry*, edited by EBSWORTH, E. A., MADDOCK, A. G. & SHARPE, A. G. Cambridge Univ. Press.
- MEESTER, P. DE, FLETCHER, S. R. & SKAPSKI, A. C. (1973). *J. Chem. Soc.* pp. 2575–2578.
- MOROSIN, B. (1966). *J. Chem. Phys.* **44**, 252–257.
- MOROSIN, B. (1970). *Phys. Rev.* **B1**, 236–243.
- NORDIO, P. L., SOOS, Z. G. & McCONNELL, H. M. (1966). *Ann. Rev. Phys. Chem.* **17**, 237–260.
- OBATA, Y. (1967). *J. Phys. Soc. Japan*, **22**, 256–263.
- O'CONNOR, B. H. & MASLEN, E. N. (1966). *Acta Cryst.* **20**, 824–835.
- PEERCY, P. S., MOROSIN, B. & SAMARA, G. A. (1973). *Phys. Rev.* **B8**, 3378–3388.
- RICHARDS, P. M., QUINN, R. K. & MOROSIN, B. (1973). *J. Chem. Phys.* **59**, 4474–4477.
- STEWART, J. M. (1971). *The X-RAY System of Crystallography Program*. Computer Science Center, Univ. of Maryland.
- STEWART, R. F., DAVIDSON, E. R. & SIMPSON, W. T. (1965). *J. Chem. Phys.* **42**, 3175–3187.
- VALENTINE, J. S., SILVERSTEIN, A. J. & SOOS, Z. G. (1974). *J. Amer. Chem. Soc.* **96**, 97–103.

Acta Cryst. (1975). B31, 770

The Crystal Structures of Na_6MnCl_8 and $\text{Na}_2\text{Mn}_3\text{Cl}_8$ and Some Isostructural Compounds

BY C. J. J. VAN LOON AND D. J. W. IJDO

Gorlaeus Laboratories, Section of Solid-State Chemistry, University of Leiden, P.O. Box 75, Leiden, The Netherlands

(Received 11 September 1974; accepted 15 October 1974)

An examination of the systems NaCl-TCl_2 ($T = \text{Mg, Mn, Fe, Cd}$) has resulted in the discovery of compounds with the stoichiometries NaTCl_3 , Na_2TCl_4 , Na_6TCl_8 and $\text{Na}_2\text{T}_3\text{Cl}_8$. The former three stoichiometries crystallize in structures that had been discovered before in FeTiO_3 (ilmenite), Sr_2PbO_4 and Mg_6MnO_8 respectively. $\text{Na}_2\text{T}_3\text{Cl}_8$ represents a new structure type and has been related to the crystal structure of $\text{Cd}_2\text{Mn}_3\text{O}_8$.

Introduction

As part of a research programme on the structural relations of compounds in the system AX-TX_2 , A representing Li or Na, T a first-row transition or an alkaline-earth metal and X being Cl, Br or I, we report in this paper the structures of Na_6MnCl_8 and $\text{Na}_2\text{Mn}_3\text{Cl}_8$ and a few isostructural compounds.

Earlier we reported the crystal structure of NaMnCl_3 (van Loon & Verschoor, 1973), the stoichiometry ATX_3 attracting our main attention. Some isostructural compounds, together with the cell edges determined from powder diffraction data, will be given in this paper. The crystal structure of Na_2MnCl_4 (Goodyear, Ali & Steigmann, 1971) was confirmed to have a Sr_2PbO_4 (Trömel, 1965) structure and some other